FAILURE MECHANISM AND SEISMIC CAPACITY OF RC FRAMES WITH URM WALL CONSIDERING BEAM DEFORMATION

KIWOONG JIN
kwjin@iis.u-tokyo.ac.jp
Graduate Student, Graduate School of Eng., The University of Tokyo, Japan
HO CHOI
Institute of Industrial Science, The University of Tokyo, Japan
choiho@iis.u-tokyo.ac.jp
NORIYUKI TAKAHASHI
Institute of Industrial Science, The University of Tokyo, Japan
ntaka@iis.u-tokyo.ac.jp
YOSHIAKI NAKANO
Institute of Industrial Science, The University of Tokyo, Japan
iisnak@iis.u-tokyo.ac.jp

ABSTRACT

The objective of this study is to evaluate in- and out-of-plane seismic capacity of unreinforced masonry (URM) walls built in reinforced concrete (RC) frames. For this purpose, RC frames with unreinforced concrete block (CB) wall for typical school buildings in Korea are experimentally investigated to evaluate their failure mechanisms and seismic capacity. One-fourth scale, one-bay specimens having different boundary condition of CB walls due to beam deformation, which is considered one of important factors affecting their out-of-plane failure, are designed, and in-plane tests under cyclic loadings are carried out as a first step herein. In this paper, the failure mechanism and the load bearing capacity of overall frames due to beam deformation are discussed.

1. INTRODUCTION

In some earthquake-prone regions of Asia, Europe, and Latin America, serious earthquake damage is commonly found resulting from catastrophic building collapse. Such damaged buildings often have unreinforced masonry (URM) walls, which are considered non-structural elements in structural performance even though URM walls may interact with boundary frames as has been often found in the past damaging earthquakes.

In the past few years, the authors have conducted cyclic loading tests of full-scale reinforced concrete (RC) frames with unreinforced concrete block (CB) walls to investigate their structural characteristics including residual

seismic capacity (Nakano et al., 2005). The specimens had rigid beams above and below the CB wall, as was generally employed in other experimental researches. However, experimental studies related to the effects of boundary condition of CB walls on their out-of-plane failure due to beam deformation, as well as the following strength degradation of the frame, are necessary to fully understand their seismic capacity. For this purpose, 1/4-scale, one-bay specimens having different boundary condition of CB walls due to beam deformation, which is considered one of important factors affecting their out-of-plane failure, are designed, and in-plane tests under cyclic loadings are carried out as a first step herein.

2. OUTLINE OF EXPERIMENT

2.1 Prototype building and experimental parameters

The test specimens are designed according to the standard design of Korean school buildings (referred to as "prototype building" shown in Figure 1) in the 1980's (The Ministry of Construction and Transportation, 2002), which is the same as the full-scale test previously investigated (Nakano et al., 2005). In this study, 4 specimens having different levels of axial load (first and fourth story) and different boundary conditions of beam (rigid and flexural beam) are tested under cyclic loading. Among these specimens, test results of the 2 specimens with different boundary conditions of beam under the axial load assuming a first story are discussed in this paper.

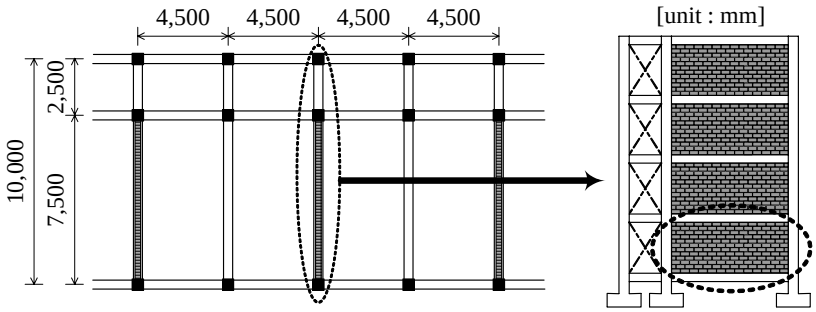

Figure 1: Standard design of Korean school buildings in the 1980's

2.2 Design of small-scale specimen

Figure 2 shows the two types of specimens. They are an infilled wall type with rigid beam (IFRB) and with flexural beam (IFFB), respectively. The design details and methods for each member are briefly described as follows.

2.2.1 *Columns and beams*

The size of column section is 1/4 of that of prototype building. The axial stress in columns, the ratio of longitudinal reinforcement, and that of shear reinforcement are almost same as the prototype building. As shown in Figure 2, the upper beam of specimen IFRB is designed to remain elastic even after the columns and CB wall fail. On the other hand, specimen IFFB

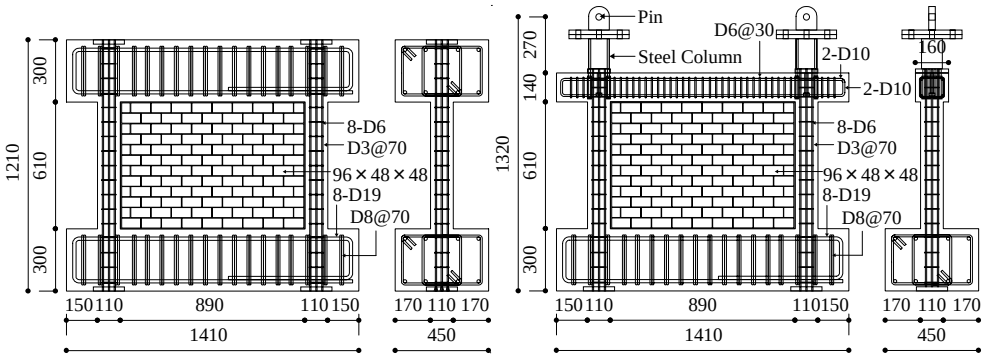

(a) *Specimen IFRB* (*b*) *Specimen IFFB*

Figure 2: Details of specimens (unit:mm)

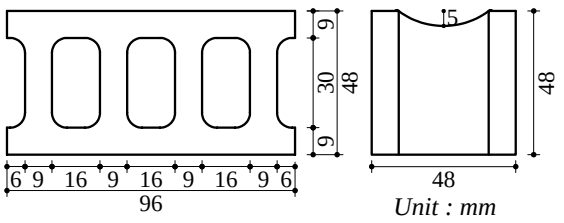

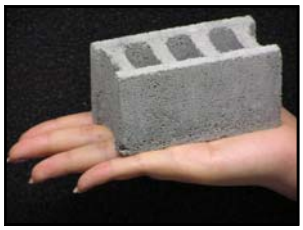

Figure 3: Details of small scale CB unit *Photo 1: Small scale CB unit*

is designed to have steel columns above the upper beam to simulate the moment distribution of the prototype building (typical 4-story building) shown in Figure 1. The upper beam with a rectangular section is designed to fail in flexure, where the shear-to-flexural strength ratio (Q_{SU} / Q_{MU}) and the maximum deflection level within elastic range are both similar to those of the prototype building.

2.2.2 *Concrete Block units*

The concrete block unit is 1/4 of that of the full-scale unit. Three layered CB prism specimens are tested, where the cement-to-sand ratio is adjusted so that the strength and stiffness should be close to those of the full-scale. It has three hollows inside and a half-sized hollow on both ends as shown in Figure 3 and Photo 1.

2.3 Material test

Tables 1 through 3 show the material test results, where the values represent the average of 3 samples in each test. Although the design strength of concrete specified in the standard design of Korean school buildings in the 1980's is 21 *MPa*, the compressive strength of test pieces exceeds the design value as shown in Table 1. The yield strength of reinforcement shows higher values by 5 to 20% than the nominal strength. The compressive strength and Young's modulus from the 3 layered CB prism tests are around 90% and 50% of the full-scale CB prism, respectively. Although the Young's modulus of CB prism is not reproduced, it is found through previous investigations according to the Equations (1) and (2) (FEMA 306, 1998) that the reduction of Young's modulus does not have much effect on the shear strength V_c of CB wall, and those 1/4-scale CB units are therefore applied to the test specimens.

Table 1: Mechanical properties of concrete (Average)

Compressive strength	Elastic modulus	Split tensile strength
30*MPa*	2.1×10^4*MPa*	2.8*MPa*

Table 2: Mechanical properties of reinforcement

Bar	Use / Member	Yield strength (*MPa*)	Tensile strength (*MPa*)	Young's modulus (*MPa*)
D3 (SD390)	Hoop / Column	420	495	1.90×10^5
D6 (SD345)	Main bar / Column	365	525	2.09×10^5
D6 (SD785)	Stirrup / Flexural beam	890	1,150	2.01×10^5
D10 (SD785)	Top main bar / Flexural beam	960	1,080	1.95×10^5
D10 (SD295)	Bottom main bar / Flexural beam	360	520	2.05×10^5

Table 3: Mechanical properties of concrete block and joint mortar

Concrete block		Joint mortar
Block prism*		
Compressive strength	Young's modulus	Compressive strength
6.5 (7.3)*MPa*	1.0 (2.0)$\times10^4$*MPa*	21.6 (20.8)*MPa*

* 3 layered specimen, ( ) : Material test results of full-scale CB unit

$$V_c = W_{eq} \cdot t \cdot f_m \cdot \cos\theta \tag{1}$$

$$W_{eq} = 0.175 \cdot \left(\frac{4 \cdot E_c \cdot I_c \cdot h_m}{E_m \cdot t \cdot \sin 2\theta \cdot h^4} \right)^{0.1} \cdot l_d \tag{2}$$

where V_c is the shear force carried by the equivalent diagonal strut of CB wall, W_{eq} is the equivalent strut width, t is the thickness of CB wall, f_m is the 50% of prism strength, θ is the angle of CB wall height to length, E_c is the Young's modulus of concrete, I_c is the moment of inertia of column, h_m is the height of CB wall, E_m is the Young's modulus of CB prism, h is the column height, and l_d is the diagonal length of CB wall, respectively. The joint mortar has the cement-to-sand ratio of 1:3.5, which is generally used in Korea and the same with the full-scale specimen (Nakano et al., 2005).

2.4 Loading plan

The loading system of specimen IFFB is shown in Figure 4. For the other specimen IFRB, a steel beam is placed between the loading beam and rigid upper beam to have the same loading point with specimen IFFB. Cyclic lateral loads are applied to each specimen through the loading beam tightly fastened to the specimen.

Figure 5 shows the loading history, where a peak drift angle (R) is defined as "lateral deformation (δ) / column height (h_0=610*mm*)". As shown in the figure, peak drift angles of 0.1, 0.2, 0.4, 0.67, 1.0, and 2.0% are planned and 2.5 cycles for each peak drift are imposed to eliminate one-sided progressive failure (unsymmetric failure pattern in positive or negative loadings). It should also be noted that 0.4% loading is imposed after 1.0% to

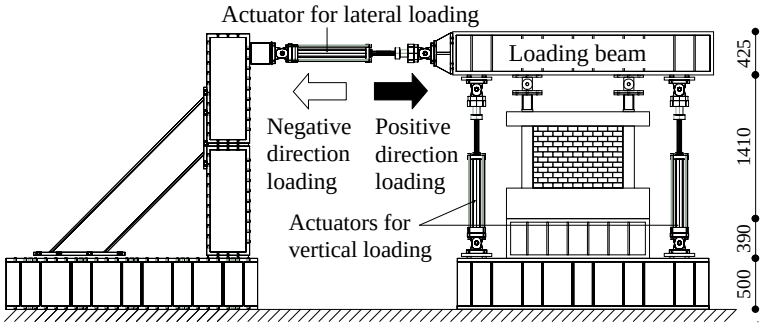

Figure 4: Test setup of specimen IFFB (Unit:mm)

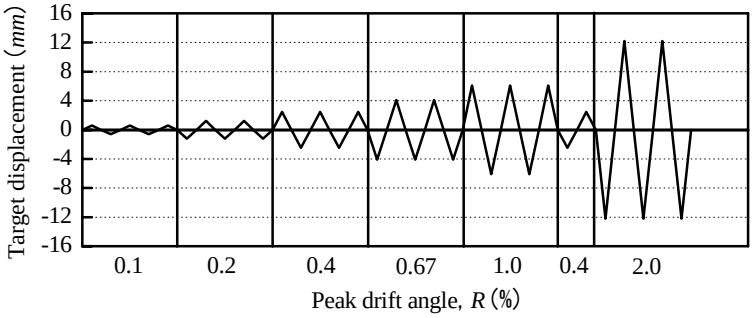

Figure 5: Loading history

investigate the effect of small amplitude loading (i.e., aftershocks) after large deformation. A constant axial load of 96*kN* is applied to each specimen.

2.5 Measurement plan

The measurement system of specimen IFFB is shown in Figure 6. The relative lateral displacement between upper and lower beams, the vertical displacement of each column, and the diagonal deformation of frame are measured. To measure the curvature distribution in columns, displacement transducers (LVDTs) are attached on both sides of each column at an interval of 150*mm*. Strains of longitudinal and shear reinforcement in columns of both specimens and in the upper beam of specimen IFFB are measured.

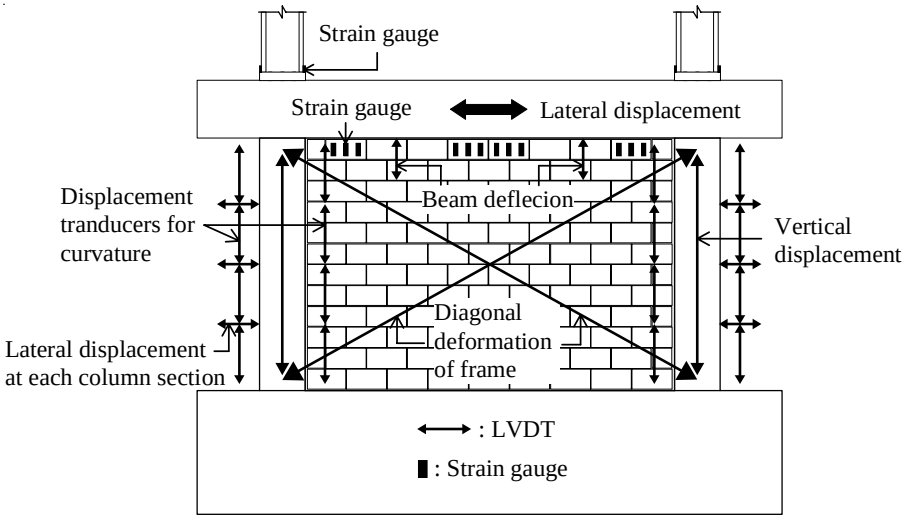

Figure 6: Measurement system (Specimen IFFB)

3. TEST RESULTS

3.1 Failure patterns

Figure 7 shows the crack patterns of both specimens at their maximum strength. The failure patterns observed in each specimen are as follows.

3.1.1 *Specimen IFRB*

Specimen IFRB has flexural cracks in RC columns and vertical and horizontal cracks in joint mortar between CB units at the first cycle with peak drift angle of +0.1%. During +0.2% loading, stair-stepped cracks in the CB wall due to diagonal strut are observed, and some cracks in joint mortar extend diagonally into CB units. Clear shear cracks at the top of tensile column and the bottom of compression column are observed at the peak drift angle of +0.4%. The crack running through the entire bed joint (horizontal joint) under the middle row of the CB wall induces slippage at the joint during -0.67% loading. Since the shear cracks at the column base of compression side rapidly open with increase in the drift angle up to -1.8%, the test is terminated during the first cycle of -1.0% loading.

3.1.2 *Specimen IFFB*

The specimen IFFB shows a failure pattern totally different from that of specimen IFRB. At the first cycle with peak drift angle of +0.1%, flexural cracks develop in columns and beam, and diagonal cracks into CB units are observed in the top row of the CB wall. Since the beam deformation causes large compressive force into the CB units at the compression corner of the wall underneath the beam, resulting in their diagonal cracks and crushing, the area of bed joint under the top row of the wall reduces and eventually the joint becomes relatively weaker than other rows. As a result, cracks causing slippage at the joint successively occur fully under the top row. It is, therefore, considered that severe damage in CB units and the following slippage at the joint caused by beam deformation imply the higher possibility of out-of-plan failure due to orthogonal excitations even in a small drift ratio. During +0.2% loading, the remaining part of CB wall under the top row acts as a diagonal strut developing stair-stepped cracks in the wall. Clear shear cracks develop in columns and beam at the peak drift angle of +0.4%. Between the peak drift angles of 0.67% and 2.0%, the damage in the beam is concentrated on its critical sections. Since the cracks at the critical sections are abruptly widened and the strains of longitudinal reinforcement in the beam significantly increase, the test is terminated at the drift angle of +3.0%.

3.2 Relation between lateral strength and drift angle

3.2.1 *Specimen IFRB*

As shown in Figure 8(a), the maximum strength of 48.6*kN* is recorded at the drift angle of +0.67% after the longitudinal reinforcement in columns yield at around +0.60%, and no remarkable strength deterioration is found

until the drift angle of +1.0%. Shear cracks at the bottom of compression column rapidly open at the drift angle of -1.0%, resulting in sudden deterioration of the lateral load carrying capacity as shown in Figure 8(a). This specimen finally fails in shear after flexural yielding in columns.

3.2.2 *Specimen IFFB*

As shown in Figure 8(b), the yielding drift angle of the longitudinal reinforcement in the upper beam is about -0.67%, and the maximum strength of 39.8*kN* is recorded at the drift angle of +1.8% after the longitudinal reinforcement in columns yield at around +1.3%. No remarkable strength deterioration is observed until the drift angle of +3.0%.

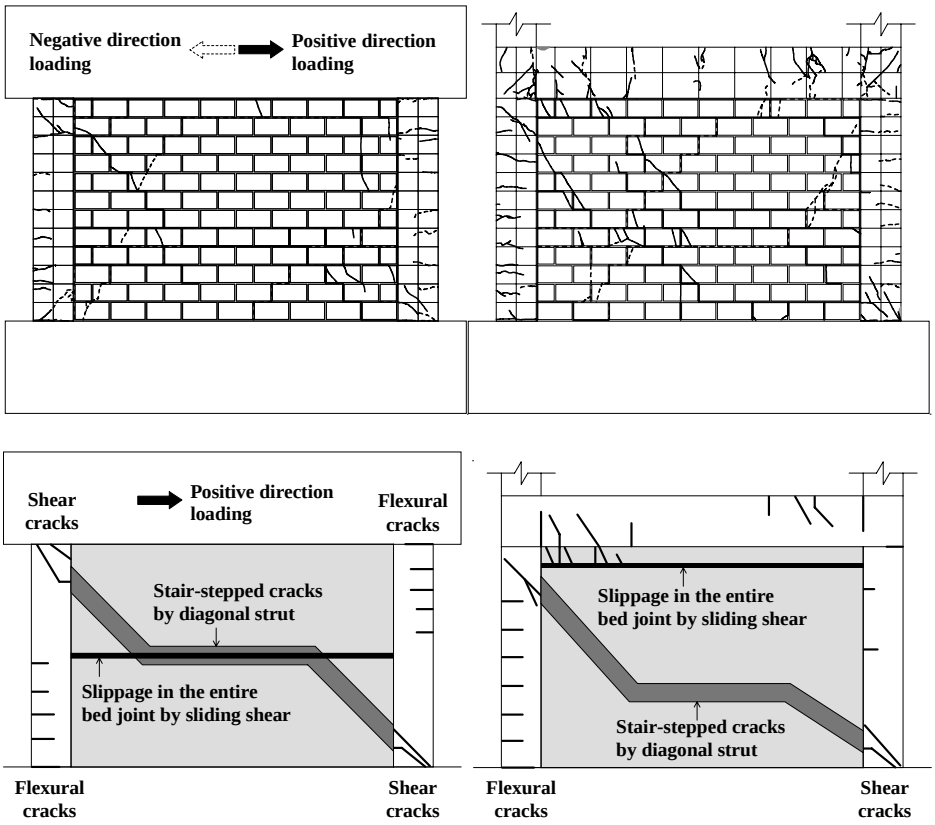

(*a*) *Specimen IFRB* (+0.67%) (*b*) *Specimen IFFB* (+2.0%)

Figure 7: Crack patterns at maximum strength

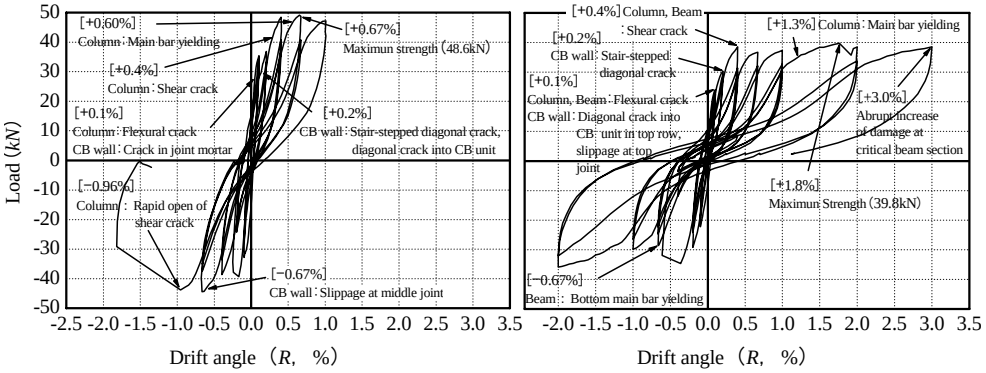

(a) Specimen IFRB *(b) Specimen IFFB*

Figure 8: Lateral strength and drift angle relation

4. MAXIMUM STRENGTH OF OVERALL FRAME

4.1 Maximum strength evaluation based on column moment distribution

4.1.1 *Specimen IFRB*

Figure 9(a) shows the curvature distribution and yield hinge zones in both columns, where measured strains of main bars exceed the yield strain. They are formed over a distance of column depth D (110mm) at both ends in each column, and their bending moment distribution assumed from the hinge formation is also shown in the figure. The flexural strength Q_{MU} (23.6kN) of each column is evaluated by $2M_U$ / 3.5D, where the ultimate bending moment M_U of columns is calculated based on the plane-section assumption setting the ultimate strain ε_{CU} at the compression fiber of concrete equal to 0.003 with an equivalent rectangular stress block coefficient 0.85. The overall lateral strength P derived from the assumptions above agrees well with the recorded capacity as shown in Figure 10 (a).

4.1.2 *Specimen IFFB*

The curvature distribution and yield hinge zones in both columns are shown in Figure 9(b). They are formed over the height of 4.0D at the bottom of tensile column and 1.0D at the bottom of compression column, respectively. The bending moment distribution assumed from the yield hinge formation is also shown in the figure. The bending moments at the beam-column joints are determined to meet the moment equilibrium, where the beam end at the top of

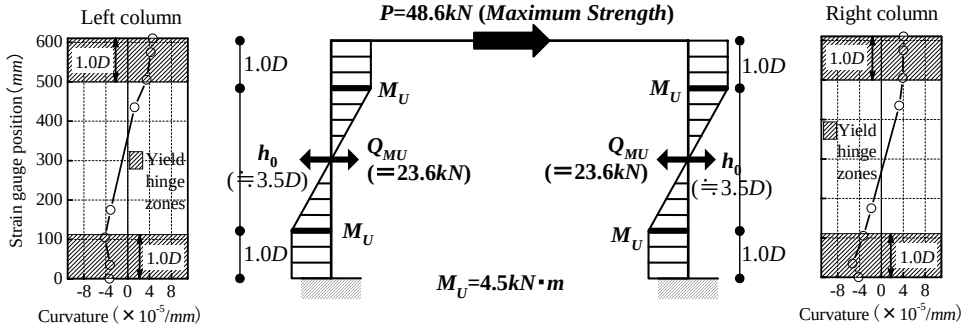

(a) Specimen IFRB

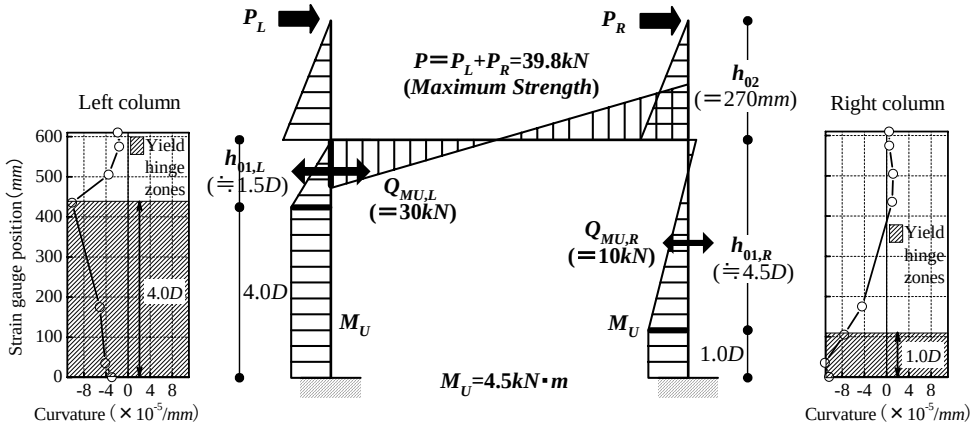

(b) Specimen IFFB

Figure 9: Curvature of columns and moment distribution at maximum strength

tensile column is assumed yielded while the moments at the bottom of upper steel columns and at the column top in compression side are derived from observed strains, which remain elastic throughout loadings. The ultimate bending moment of the beam end is calculated based on the same assumption with that of the column of specimen IFRB, where the tensile axial load (-10.5*kN*) acting in the beam is considered. The flexural strength Q_{MU} in each column is then calculated considering the rest span length (1.5*D* in the tensile column and 4.5*D* in the compression column) above yield hinge zones as shown in Figure 9(b). The overall lateral strength *P* considering the column hinge zones agrees well with the recorded capacity as shown in Figure 10(b).

4.2 Maximum strength estimation by practical method

In the previous section, the overall lateral strengths of RC frames with CB wall are evaluated according to the observed moment (or curvature) distribution in columns. In the design stage, however, the moment distribution discussed earlier based on the curvature profile is not given and the lateral strength can not be predicted as is done in this study. A simplified strength

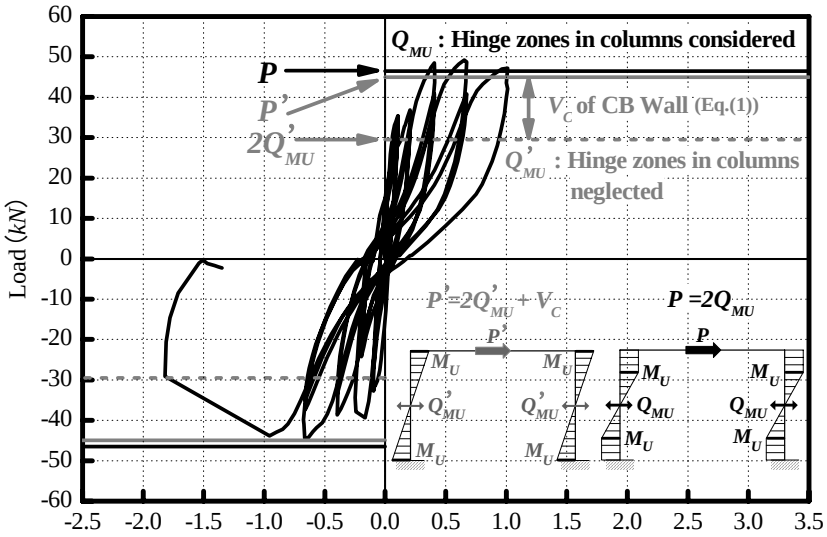

(a) Specimen IFRB

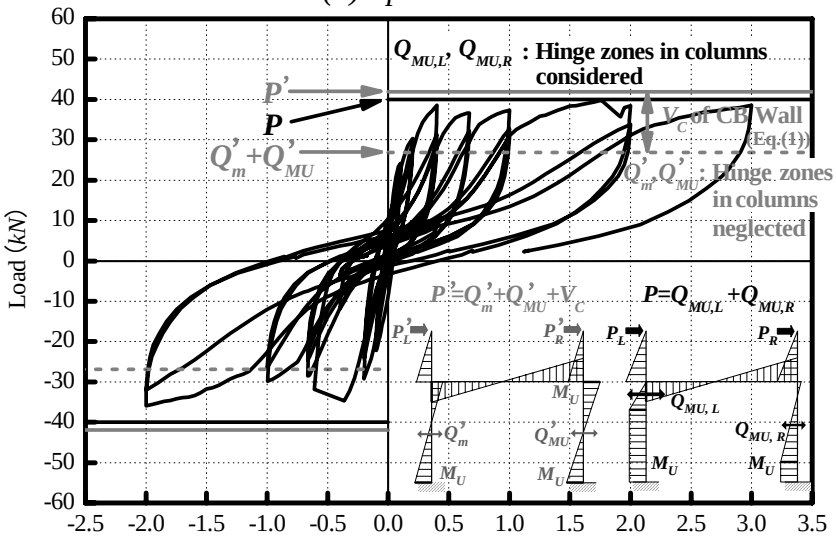

(*b*) *Specimen IFFB*

Figure 10: Maximum strength of overall frame

evaluation of the specimens is, therefore, made based on the FEMA 306 (1998), where the strength is calculated from column moments neglecting hinge zones resulting from the presence of CB wall.

In the simplified evaluation, the ultimate strength of the bare frame is first calculated, and the shear force V_C contributed by CB wall is then added to the strength above to obtain the overall strength. For specimen IFRB, as shown in Figure 10(a), yield hinges are assumed at both column ends, and the column strength Q'_{MU} is computed by $2M_U$ / 610*mm* (column height), where M_U is defined in subsection 4.1.1. For specimen IFFB, as shown in Figure 10(b), the column strength Q'_{MU} in compression side is obtained by the same assumption with that of specimen IFRB, while the yield hinge is assumed both at the beam end and at the column bottom to obtain the strength Q'_m in tensile side. The ultimate bending moment at beam end, where the tensile axial load (-2.3*kN*) acting in the beam is not taken into account for the practical estimation because of its negligible effect on the beam strength and accordingly column strength, is distributed to the top of tensile column in accordance with the elastic moment distribution ratio at its top and the bottom of steel column. The shear force V_C (15*kN* for both specimens) of CB wall carried by the equivalent diagonal strut is computed by Equation (1) (FEMA 306, 1998). The sum of shear forces of the bare frames and CB walls, plotted in Figure 10, shows good agreement with the recorded maximum strength of overall frames in both specimens.

5. CONCLUSIONS

Seismic performance of RC frames with unreinforced CB wall for standard Korean school buildings were experimentally investigated under cyclic loadings. The major findings can be summarized as follows.

(1) Because of beam deformation above CB wall and resulting different yield hinge zones, the moment distribution in columns and load bearing capacity of specimen IFFB are totally different from those of specimen IFRB. It should also be noted that severe damage in CB units and slippage at the joint is developed in the early stage of loading due to beam deformation in specimen IFFB, and it implies the higher possibility of out-of-plan failure even in a small drift ratio when the beam is not fully rigid.
(2) The maximum strength evaluated by the moment distribution along columns considering hinge zones agrees well with the load bearing capacity recorded in both specimens.
(3) A simplified method consisting of the bare frame strength neglecting hinge zones and the contribution of CB wall computed based on FEMA 306 (1998) can successfully predict the load bearing capacity of overall frame.

REFERENCES

The Ministry of Construction and Transportation, 2002. A Study on the Seismic Evaluation and Retrofit of Low-Rise RC Buildings in Korea (in Korean).

Nakano, Y. and Choi, H., 2005. Experimental Study on Seismic Behavior and Crack Pattern of Concrete Block Infilled RC Frames. *New Technologies for Urban Safety of Mega Cities in Asia (USMCA)*, ICUS/INCEDE Report 2, Singapore.

FEMA 306, 1998. *Evaluation of Earthquake Damaged Concrete and Masonry Wall Buildings*. Applied Technology Council (ATC-43 Project).